

ORIGINAL RESEARCH

Analysis of the drug-target-disease network of trichosanthes-angelica sinensis-frankincense-myrrh in the treatment of breast cancer

Jinqing Yang^{1,†}, Xiaochun Zhang^{1,†}, Zhiwei Jiang², Zhengming Deng², Jinhai Tang^{1,3,*}

¹The First Clinical Medical College, Nanjing University of Chinese Medicine, 210023 Nanjing, Jiangsu, China

²Department of General Surgery, Jiangsu Provincial Hospital of Traditional Chinese Medicine, the Affiliated Hospital of Nanjing University of Chinese Medicine, 210023 Nanjing, Jiangsu, China.

³Department of General Surgery, The First Affiliated Hospital with Nanjing Medical University, 210029 Nanjing, Jiangsu, China

***Correspondence**

jhtang@njmu.edu.cn
(Jinhai Tang)

† These authors contributed equally.

Abstract

This study aims to investigate the key bioactive compounds, potential targets, and molecular mechanisms of Trichosanthes-Angelica sinensis-Frankincense-Myrrh (TAFM) in the treatment of breast cancer using network pharmacology and molecular docking methods. The chemical constituents and related targets of TAFM were obtained using the Traditional Chinese Medicine Systems Pharmacology Database and Analysis Platform (TCMSP) database. GeneCards, Online Mendelian Inheritance in Man (OMIM), Drugbank, and Therapeutic Target Database (TTD) databases were used to identify breast cancer-related targets. Cytoscape 3.9.1 software and the STRING (Search Tool for the Retrieval of Interaction Gene/Proteins) database were used to visualize the drug component-target-disease and protein interaction networks before screening the core components and key targets. Gene Ontology (GO) and Kyoto Encyclopedia of Genes and Genomes (KEGG) analyses were performed using the DAVID (Database for Annotation, Visualization and Integrated Discovery) database, and molecular docking was performed using AutoDock and PyMOL software. We found that the key active ingredients of TAFM in the treatment of breast cancer include β -sitosterol, stigmaterol, ellagic acid, pelargonidin, and petunidin. A total of 38 key targets and hub genes, including *ESR1*, *VEGFA*, *PTGS2*, *HSP90AA1*, and *CASP3*, were identified. Molecular docking results confirmed that stigmaterol and Caspase 3 (*CASP3*) were the most closely related targets. GO enrichment analysis demonstrated that the biological processes involved mainly included drug response, positive apoptosis process regulation, and two-way gene expression regulation. KEGG pathway analysis revealed the involvement of pathways related to cancer, inflammation, and infection-related diseases. The study results provide supportive evidence that β -sitosterol, stigmaterol, ellagic acid, pelargonidin, and petunidin represent the key bioactive ingredients of TAFM that exhibit anti-breast cancer activity through the regulation of estrogen receptor alpha (*ESR1*), vascular endothelial growth factor A (*VEGFA*), prostaglandin-endoperoxide synthase 2 (*PTGS2*), heat shock protein 90 alpha (*HSP90AA1*), and *CASP3* in the treatment of breast cancer.

Keywords

Molecular docking; Breast cancer; Network pharmacology; Trichosanthes-angelica sinensis-frankincense-myrrh

1. Introduction

Although cancer-related research has made great progress, breast cancer remains the most common cancer affecting the health of women worldwide. Breast cancer is the leading cause of cancer deaths, accounting for 25% of cancer diagnoses and 15% of female cancer deaths [1, 2]. Although breast cancer can be comprehensively treated by surgery, radiotherapy and chemotherapy, immunotherapy, hormones, and targeted therapy, which has improved the prognosis of patients with breast cancer, many deficiencies remain, and a high probability of

recurrence and metastasis is noted [2]. Therefore, there is an urgent need to identify more effective treatment measures and reveal their underlying antitumour mechanisms to provide new insights into breast cancer treatment.

Numerous experiments and clinical studies have demonstrated the beneficial treatment effects of traditional Chinese medicine on breast cancer based on syndrome differentiation, especially in the treatment of postoperative radiotherapy and chemotherapy patients [3–6]. Traditional Chinese medicine can effectively inhibit tumour recurrence and metastasis, promote postoperative rehabilitation, and enhance the quality of

life of patients [3, 7]. The Trichosanthes-Angelica sinensis-Frankincense-Myrrh (TAFM) Chinese herb combination is derived from the classic prescription book “Liang Fu Fang” from the Song Dynasty. This agent is currently commonly and effectively used in the clinical treatment of breast carbuncles, breast cancer, and diarrhoea. In the system of traditional Chinese medicine, Trichosanthes (Gua Lou) is applied to eliminate phlegm and promote blood circulation. In addition, Angelica sinensis (Dang Gui) can replenish blood circulation, whereas frankincense (Ru Xiang) and myrrh (Mo Yao) both regulate qi and activate blood circulation. All the drugs are used together to soothe the liver, relieve depression, dissipate knots, and eliminate symptoms closely associated with the pathogenesis of breast cancer according to the classical theory of traditional Chinese medicine. However, there is no systematic research or clear explanation of the mechanisms associated with this prescription in the treatment of breast cancer.

Network pharmacology has made great progress in the past decade. This methodology is efficiently used to study the interactions among drugs, targets, and diseases and can be employed to screen the effective components and targets of herbal medicine. In this study, we used network pharmacology and molecular docking methods to construct a drug-target-disease network to reveal the potential mechanisms of the combination of TAFM in the treatment of breast cancer as displayed in Fig. 1. This study provides a reference for further experimental research on the treatment of breast cancer using TAFM.

2. Methods

2.1 Collection of the active extracts and targets of TAFM

The components of Trichosanthes, Angelica sinensis, Frankincense, and Myrrh from the TCMSP (Traditional Chinese Medicine Systems Pharmacology Database and Analysis Platform, <https://old.tcm-sp-e.com/tcm-sp.php>) were collected [8] and selected according to the following screening criteria: oral bioavailability (OB) $\geq 30\%$ and drug-likeness (DL) ≥ 0.18 . The OB describes the percentage of the oral drug absorbed by the gastrointestinal tract that reaches the systemic circulation through the liver. DL refers to the structural similarity between herbal ingredients and known drugs. The targets were transformed into standard gene names using the UniProt database (Unified Protein Database, <https://www.uniprot.org/uploadlists/>). Verified protein data were selected, and the species source was set as human.

2.2 Acquisition of breast cancer targets

Breast cancer-related targets were acquired from the GeneCards (<https://www.genecards.org/>) [9], OMIM (<https://www.omim.org/>) [10], TTD (<http://db.idrblab.net/ttd/>) [11], and DrugBank (<https://go.drugbank.com>) [12] databases. We used the Venny 2.1 online tool to determine the intersection of TAFM and breast cancer-related targets by creating a Venn diagram.

2.3 Drug-target-disease network

We imported the active ingredients and action targets of TAFM into Cytoscape 3.9.1 software (National Institute of General Medical Sciences, USA) and generated the network diagram of “drugs-active ingredients-targets-diseases”. The nodes represent the acting drugs, active ingredients, targets, and breast cancer, and the edges represent the interactions among the nodes. In addition, the importance of degree centrality (degree value) was determined for the response nodes.

2.4 Protein-protein interaction (PPI) network

We input the targets overlapping between TAFM and breast cancer into the STRING database (<https://string-db.org/>) [13], selected the species as human, and set the maximum confidence level to ≥ 0.7 . Furthermore, we used Cytoscape 3.9.1 to visualize and analyse the PPI network and chose the degree parameter as the screening condition of the core node. The node with a degree value greater than twice the median value was regarded as the core node in the network.

2.5 Gene Ontology (GO) and Kyoto Encyclopedia of Genes and Genomes (KEGG) enrichment analysis

We used the DAVID database (<https://david.ncifcrf.gov/>) [14] to upload the intersection target, defined the species as Homo sapiens, and conducted GO and KEGG functional enrichment analyses, including molecular function (MF), biological process (BP), and cellular component (CC) analyses. Then, we identified potential biological processes and signalling pathways involved in TAFM against breast cancer based on a p value < 0.05 .

2.6 Molecular docking

We used the molecular docking method to verify the correlation between the main active components of TAFM and core target proteins. The 3D structure of the target protein was obtained from the Protein Data Bank (PDB) database (<https://www.rcsb.org/>) [15], and that of the key compound was obtained from the TCMSP and PubChem databases (<https://pubchem.ncbi.nlm.nih.gov/>) [16] and converted to the PDB format using PyMOL 2.5 software (San Carlos, CA, USA). PyMOL software was used to remove water from the target protein and the additional ligand structure, and then Autodock 1.5.7 software (Scripps Research, La Jolla, CA, USA) was used to add hydrogen atoms to the active ingredients and target protein, combine nonpolar hydrogen atoms, calculate the charge number, build docking pockets, and verify the molecular docking. Finally, the docking results were graphed using PyMOL software. The study showed that the binding energy was less than -4.25 kcal/mol, indicating that the compound exhibited good binding to the target [17].

3. Results

TABLE 1. Active ingredients of *Trichosanthes-Angelica sinensis-Frankincense-Myrrh* (TAFM).

Source	MOLID	Active component	OB	DL
Trichosanthes	MOL007180	Vitamin E	32.29	0.70
Trichosanthes	MOL004355	Spinasterol	42.98	0.76
Trichosanthes	MOL006756	Schottenol	37.42	0.75
Trichosanthes	MOL001494	Mandenol	42.00	0.19
Trichosanthes	MOL007179	Linolenic acid ethyl ester	46.10	0.20
Trichosanthes	MOL007175	Karounidiol 3-o-benzoate	43.99	0.50
Trichosanthes	MOL005530	Hydroxygenkwanin	36.47	0.27
Trichosanthes	MOL002881	Diosmetin	31.14	0.27
Trichosanthes	MOL007172	7-Oxo-dihydrokaro-unidiol	36.85	0.75
Trichosanthes	MOL007171	5-Dehydrokarounidiol	30.23	0.77
Trichosanthes	MOL007165	10 α -Cucurbita-5, 24-diene-3 β -ol	44.02	0.74
Angelica sinensis	MOL000358	Beta-sitosterol	36.91	0.75
Angelica sinensis & Myrrh	MOL000449	Stigmasterol	43.83	0.76
Frankincense	MOL001272	Incensole	45.59	0.22
Frankincense	MOL001295	Phyllocladene	33.4	0.27
Frankincense	MOL001265	Acetyl-alpha-boswellic acid	42.73	0.70
Frankincense	MOL001241	O-acetyl- α -boswellic acid	42.73	0.70
Frankincense	MOL001215	Tirucallol	42.12	0.75
Frankincense	MOL001255	Boswellic acid	39.55	0.75
Frankincense	MOL001243	3 α -Hydroxy-olean-12-en-24-oic-acid	39.32	0.75
Frankincense	MOL001263	3-Oxo-tirucallic, acid	42.86	0.81
Myrrh	MOL001001	Quercetin-3-O- β -D-glucuronide	30.66	0.74
Myrrh	MOL001002	Ellagic acid	43.06	0.43
Myrrh	MOL001004	Pelargonidin	37.99	0.21
Myrrh	MOL001006	Poriferasta-7, 22E-dien-3 β -ol	42.98	0.76
Myrrh	MOL001009	Guggulsterol-VI	54.72	0.43
Myrrh	MOL001013	Mansumbinoic acid	48.10	0.32
Myrrh	MOL001019	(7S, 8R, 9S, 10R, 13S, 14S, 17Z)-17-Ethylidene-7-hydroxy-10, 13-dimethyl-1, 2, 6, 7, 8, 9, 11, 12, 14, 15-Decahydrocyclopenta (a) phenanthrene-3, 16-dione	35.75	0.48
Myrrh	MOL001021	7 β , 15 β -Dihydroxypregn-4-ene-3,16-dione	43.11	0.51
Myrrh	MOL001022	11 α -Hydroxypregna-4, 17(20)-trans-diene-3, 16-dione	36.62	0.47
Myrrh	MOL001026	Myrrhanol C	39.96	0.58
Myrrh	MOL001027	Myrrhanone A	40.25	0.63
Myrrh	MOL001028	(8R)-3-Oxo-8-hydroxy-polypoda -13E, 17E, 21-triene	44.83	0.59
Myrrh	MOL001029	Myrrhanones B	34.39	0.67
Myrrh	MOL001031	Epimansumbinol	61.81	0.40
Myrrh	MOL001033	Diayangambin	63.84	0.81
Myrrh	MOL001040	(2R)-5, 7-Dihydroxy-2-(4-hydroxyphenyl) chroman-4-one	42.36	0.21

TABLE 1. Continued.

Source	MOLID	Active component	OB	DL
Myrrh	MOL001045	(13 <i>E</i> , 17 <i>E</i> , 21 <i>E</i>)-8-Hydroxypolypodo-13, 17, 21-trien-3-one	44.34	0.58
Myrrh	MOL001046	(13 <i>E</i> , 17 <i>E</i> , 21 <i>E</i>)-Polypodo-13, 17, 21-triene-3, 18-diol	39.96	0.58
Myrrh	MOL001049	16-Hydroperoxymansumbin-13 (17)-en-3 β -ol	41.05	0.49
Myrrh	MOL001052	Mansumbin-13 (17)-en-3, 16-dione	41.78	0.45
Myrrh	MOL001061	(16 <i>S</i> , 20 <i>R</i>)-Dihydroxydammar-24-en-3-one	37.34	0.78
Myrrh	MOL001062	15 α -Hydroxymansumbinone	37.51	0.44
Myrrh	MOL001063	28-Acetoxy-15 α -hydroxymansumbinone	41.85	0.67
Myrrh	MOL001069	3 β -Acetoxy-16 β , 20(<i>R</i>)-dihydroxydammar-24-ene	38.72	0.81
Myrrh	MOL001088	1 α -Acetoxy-9, 19-cyclolanost-24-en-3 β -ol	44.4	0.78
Myrrh	MOL001092	((3 <i>R</i> , 5 <i>R</i> , 8 <i>R</i> , 9 <i>R</i> , 10 <i>R</i> , 13 <i>R</i> , 14 <i>R</i> , 17 <i>S</i>)-17-((2 <i>S</i> , 5 <i>S</i>)-5-(2-Hydroxypropan-2-yl)-2-methyloxolan-2-yl)-4, 4, 8, 10, 14-pentamethyl-2, 3, 5, 6, 7, 9, 11, 12, 13, 15, 16, 17-dodecahydro-1H-cyclopenta (a) phenanthren-3-yl) acetate	33.07	0.80
Myrrh	MOL001093	Cabraleone	36.21	0.82
Myrrh	MOL001095	Isofouquierone	40.95	0.78
Myrrh	MOL001126	((5 <i>aS</i> , 8 <i>aR</i> , 9 <i>R</i>)-8-oxo-9-(3, 4, 5-Trimethoxyphenyl)-5, 5 <i>a</i> , 6, 9-tetrahydroisobenzofurano (6, 5- <i>f</i>) (1, 3) benzodioxol-8 <i>a</i> -yl) acetate	44.08	0.90
Myrrh	MOL001131	Phellamurin-qt	56.60	0.39
Myrrh	MOL001138	(3 <i>R</i> , 20 <i>S</i>)-3, 20-Dihydroxydammar-24-ene	37.49	0.75
Myrrh	MOL001145	(20 <i>S</i>)-3 β -Acetoxy-12 β , 16 β , 25-tetrahydroxydammar-23-ene	34.89	0.82
Myrrh	MOL001146	(20 <i>S</i>)-3 β , 12 β , 16 β , 25-Pentahydroxydammar-23-ene	37.94	0.75
Myrrh	MOL001147	(20 <i>R</i>)-3 β -Acetoxy-16 β -dihydroxydammar-24-ene	40.36	0.82
Myrrh	MOL001148	3 β -Hydroxydammar-24-ene	40.27	0.82
Myrrh	MOL001156	3-Methoxyfuranoguaia-9-en-8-one	35.15	0.18
Myrrh	MOL001164	((5 <i>S</i> , 6 <i>R</i> , 8 <i>R</i> , 9 <i>Z</i>)-8-Methoxy-3, 6, 10-trimethyl-4-oxo-6, 7, 8, 11-tetrahydro-5H-cyclodeca (b) furan-5-yl) acetate	34.76	0.25
Myrrh	MOL001175	Guggulsterone	42.45	0.44
Myrrh	MOL000490	Petunidin	30.05	0.31
Myrrh	MOL000979	2-Methoxyfuranoguaia-9-ene-8-one	66.18	0.18
Myrrh	MOL000988	4, 17(20)-(cis)-Pregnadiene-3, 16-dione	51.42	0.48
Myrrh	MOL000996	Guggulsterol IV	33.59	0.74
Myrrh	MOL001093	Cabraleone	36.21	0.82
Myrrh	MOL001095	Isofouquierone	40.95	0.78

OB, oral bioavailability; DL, drug-like; MOL ID: molecular ID.

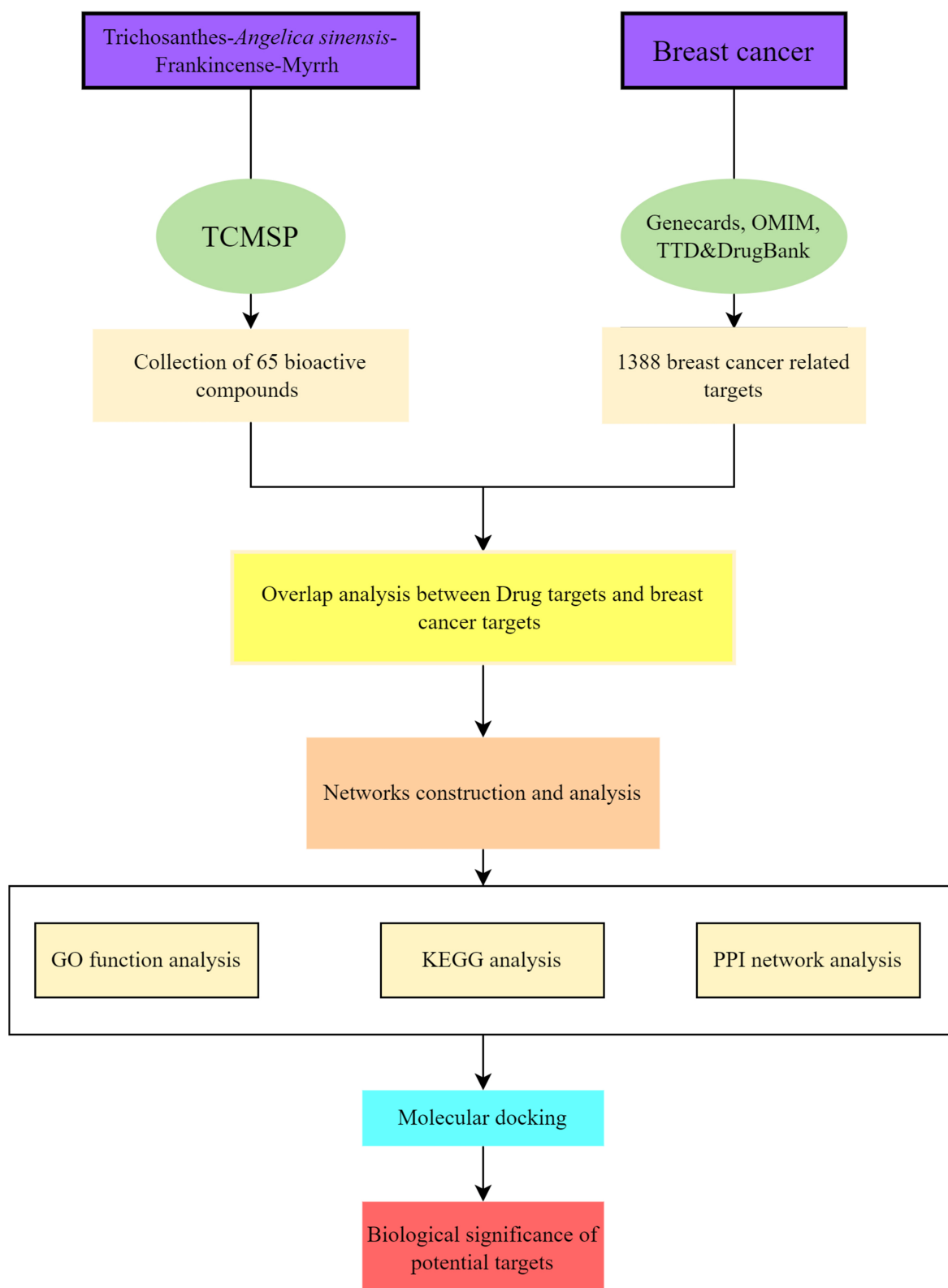


FIGURE 1. Workflow of the study. TCMSP: Traditional Chinese Medicine Systems Pharmacology Database and Analysis Platform; GO: Gene Ontology; KEGG: Kyoto Encyclopedia of Genes and Genomes; OMIM: Online Mendelian Inheritance in Man; TTD: Therapeutic Target Database; PPI: Protein-protein interaction.

3.1 Active components and action targets of TAFM

The active components of TAFM were searched in the TCMSP according to the search conditions described above. After

removing the duplicate items, 65 active components and 91 targets were screened (Table 1). Stigmasterol is the common active ingredient of *Angelica sinensis* and myrrh.

3.2 Search for potential targets of TAFM in the treatment of breast cancer

A total of 1388 breast cancer-related targets were obtained by merging the targets from the GeneCards, OMIM, TTD, and Drugbank databases and deleting duplicates. In total, 806 potential targets of breast cancer were obtained from the GeneCards database with a relevance score >20 according to the median relevance score setting, 535 targets were obtained from the OMIM database, 102 targets were obtained from the Drugbank database, and 138 targets were obtained from the TTD database. We then used a Venn diagram to identify the intersection between TAFM and related breast cancer targets. Finally, 38 potential targets of TAFM for breast cancer treatment were obtained (Fig. 2).

Breast cancer Drug targets

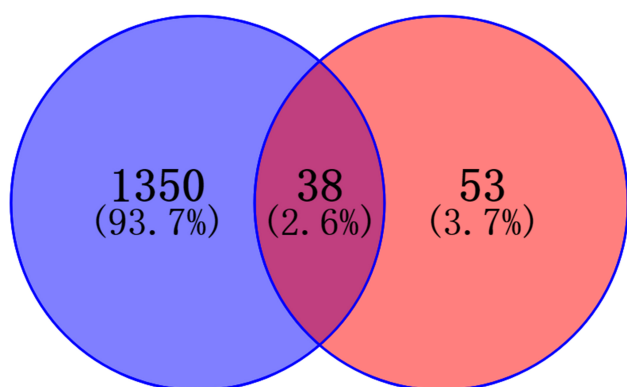


FIGURE 2. Venn diagram of the targets of the active ingredients of TAFM and breast cancer-related targets.

3.3 Protein-protein interaction network and hub genes

To explore which key drug targets played a major role, we built a PPI network by uploading overlapping targets of TAFM and breast cancer from the STRING database (Fig. 3A), and Cytoscape 3.9.1 software was used to visualise the interactions. There were 38 targets and 281 edges. We then ran the cytoHub app to further identify the hub genes (Fig. 3B), which appeared as red nodes in the network. The top five targets according to degree value ranking include estrogen receptor alpha (ESR1), vascular endothelial growth factor A (VEGFA), pros-taglandin-endoperoxide synthase 2 (PTGS2), heat shock protein 90 alpha (HSP90AA1), and Caspase 3 (CASP3) which may play important regulatory roles in the treatment of breast cancer.

3.4 KEGG and GO function analysis

To reveal the potential mechanism of TAFM in breast cancer treatment, we performed KEGG and GO functional analyses. The GO function enrichment results revealed the involvement of 326 biological processes, including 238 biological processes (BP), 27 cell component expression processes (CC), and 61 molecular function-related processes (MF) ($p < 0.05$). The top ten items of BP, CC and MF are displayed in the enrichment

analysis bubble chart. The targets generally consist of the positive regulation of drug response, apoptosis process, and two-way regulation of gene expression (BP); cytoplasm, nucleus, mitochondria (CC); and enzyme binding, same protein binding, steroid binding (MF) (Fig. 4A). The KEGG results demonstrated the involvement of 103 signalling pathways, including hepatitis B, lipid and atherosclerosis, Kaposi sarcoma-associated herpesvirus infection, IL-17 signalling pathway, and chemical carcinogenesis-receptor activation (Fig. 4B).

3.5 Network of traditional Chinese medicine-active ingredients-targets-diseases

We used Cytoscape 3.9.1 software to generate the traditional Chinese medicine-active ingredients-targets-diseases network (Fig. 5). The network of 38 overlapping targets was composed of 82 nodes and 191 edges. TAFM exerts anti-breast cancer effects through multiple components and targets. The cytonca plug-in was used to obtain the components with the highest degree values. The results indicated that β -sitosterol, stigmaterol, ellagic acid, pelargonidin, and petunidin potentially represent the key active ingredients of TAFM in the treatment of breast cancer (Table 2).

3.6 Molecular docking

It is widely believed that an absolute binding energy of >4.25 kcal/mol indicates an interaction between molecules and the target activity, and a strong binding activity is noted for values of >7.0 kcal/mol, which indicates that the ligand and protein can form a stable structure [17]. Molecular docking results suggest the possibility of binding between all key ingredients and core proteins encoded by hub genes (Table 3). In particular, stigmaterol potentially stably binds to ESR1 (PDB ID: 1GWQ), VEGFA (PDB ID: 4KZN), CASP3 (PDB ID: 3DEI), and HSP90AA1 (PDB ID: 1BYQ) with binding energies was less than -7.0 kcal/mol. Similarly, CASP3 and β -sitosterol, ESR1, PTGS2 (PDB ID: 5F19), ellagic acid, PTGS2, and pelargonidin pigment also exhibit stable binding. The stable bindings were visualized using PyMOL software (Fig. 6A-E).

4. Discussion

Traditional Chinese medicine has been extensively researched and is an important source of drugs for clinical use [18, 19]. However, the multicomponent and multitarget nature of traditional Chinese medicines, as well as the diverse regulatory mechanisms involved in their activities, make it difficult to identify the key components and complex interactions of these formulas. Network pharmacology is an advanced, efficient, and suitable method for systematically studying traditional Chinese medicine compounds [20–22]. To the best of our knowledge, the present study is the first to predict the potential active molecules, targets, and mechanisms of traditional Chinese medicine compounds (TAFM) acting on breast cancer by constructing a traditional Chinese medicine-active ingredients-targets-diseases network and performing molecular docking. This study provides a new perspective for breast cancer treatment and a research direction for the precise treatment of

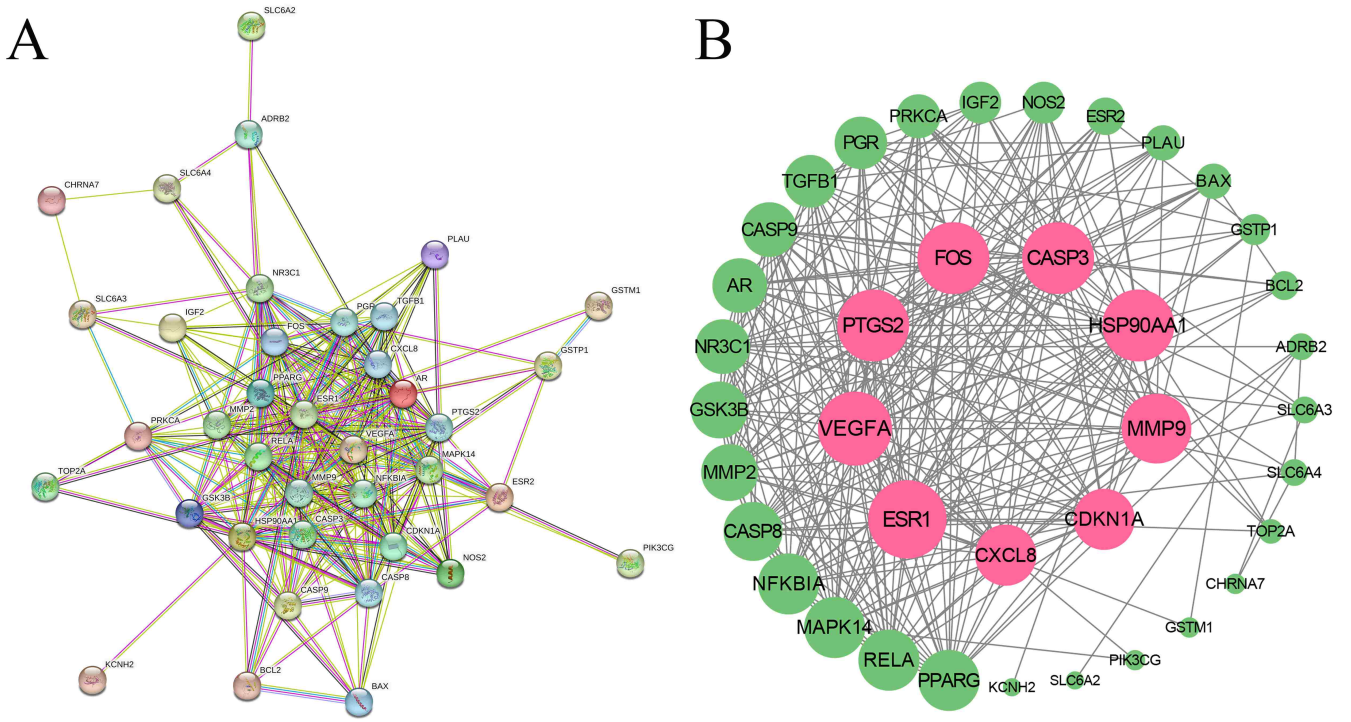


FIGURE 3. PPI network and hub genes of TAFM in breast cancer treatment. Each node represents a related target gene. (A) PPI network of the common targets from the STRING database. (B) Hub genes were identified using Cytoscape software. The degree of the green nodes (genes) was relatively lower, and the red nodes represent the hub genes with high degree values.

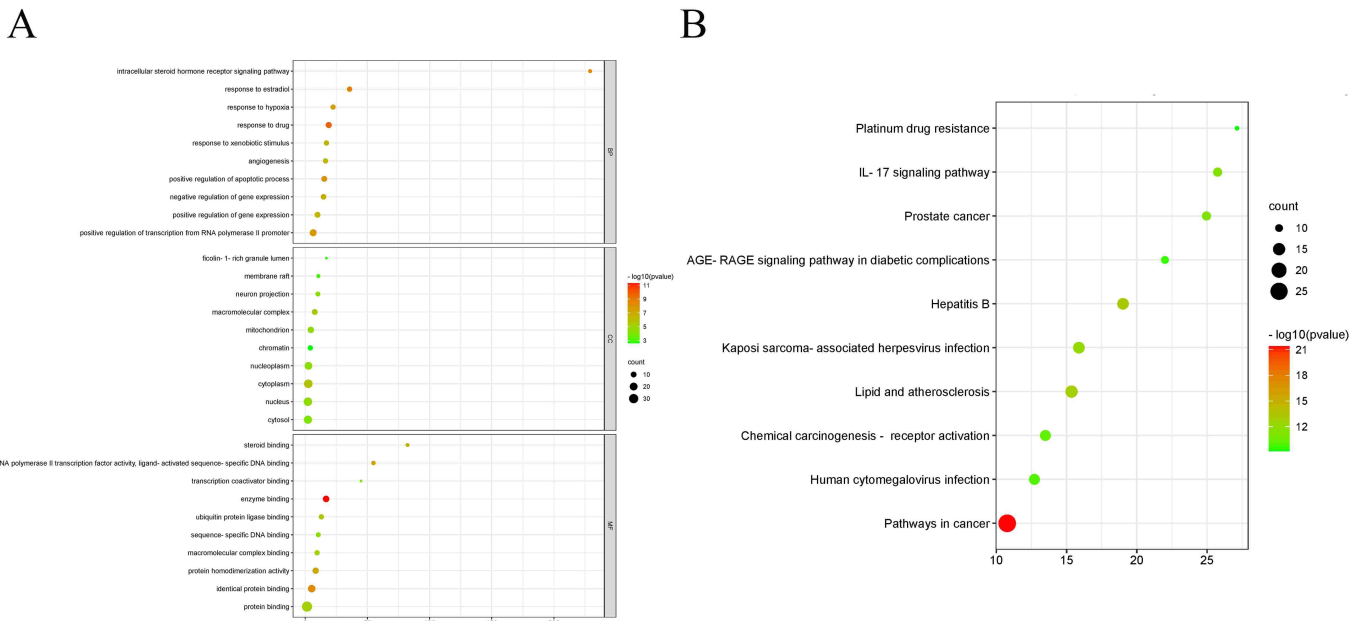


FIGURE 4. Bubble diagram of GO and KEGG analysis. The size of the dot represents the number of enriched targets. Different colours represent a different p value ($-\log_{10}$).

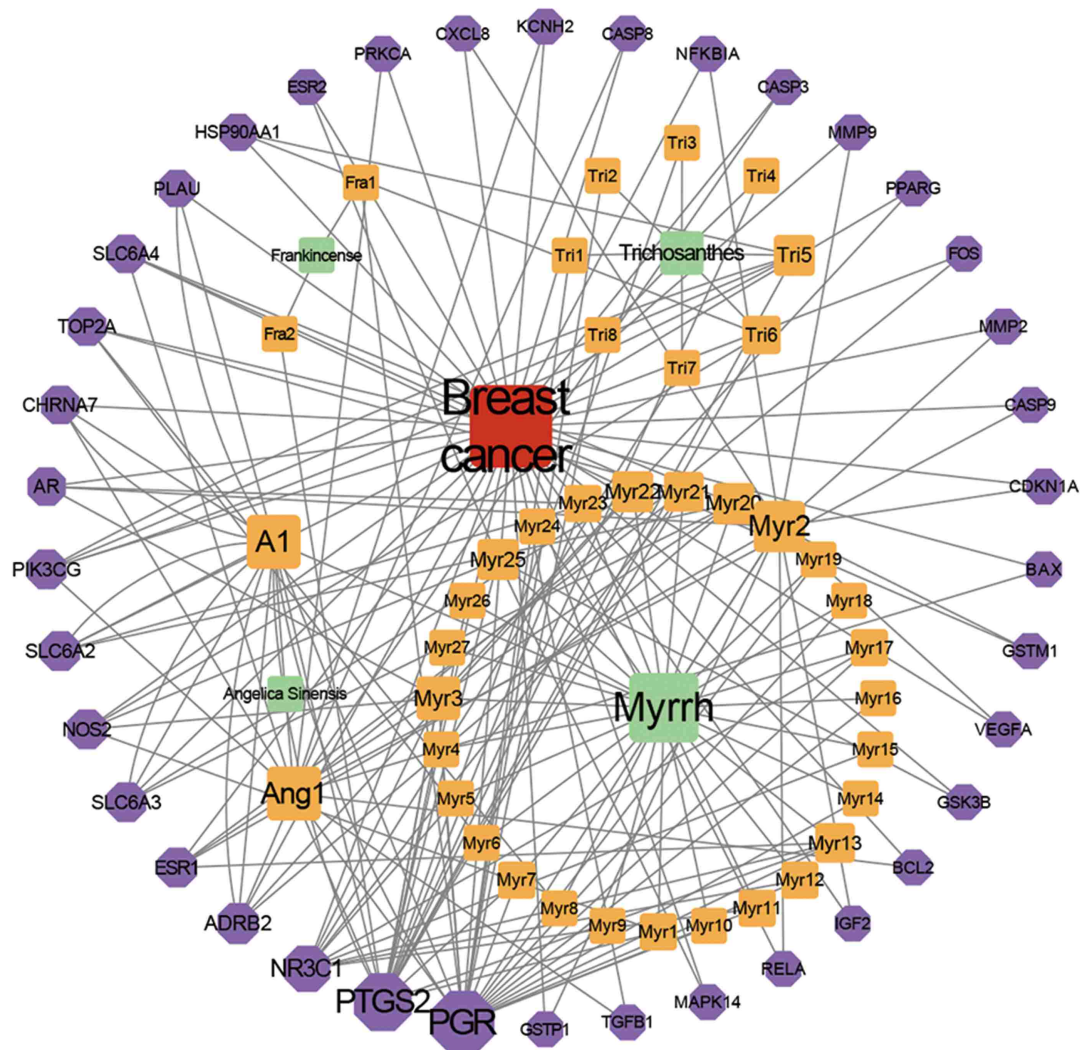


FIGURE 5. Traditional Chinese Medicine-active ingredients-targets-diseases interaction network. Green nodes represent traditional Chinese medicine compounds (T-A-F-M), and orange nodes represent bioactive ingredients. A1 represents the common compound. Purple hexagons represent common targets, and red squares represent diseases.

cancer using traditional Chinese medicine compounds.

Molecular docking is an important technology that predicts the binding mode and affinity of targets and candidate drugs to realize structure-based drug design [23–25]. Our study showed that the key active ingredients of TAFM, including β -sitosterol, stigmasterol, ellagic acid, pelargonidin, and petunidin, potentially stably bind to core proteins encoded by hub genes and confirmed that the potential active components identified from extracts are reliable. In addition, molecular docking provides a research direction for drug development and therapy targets. Many studies have revealed that these key active molecules exhibit anti-breast cancer activity. As an effective apoptosis promoter, high β -sitosterol concentrations significantly inhibit the proliferation of human breast cancer T47D and MDA-MB-231 cells [26–29]. Stigmasterol and β -sitosterol are similar to cholesterol in structure and are classified as phytosterols [30]. Stigmasterol promotes cancer apoptosis by inducing reactive oxygen species production and calcium overload and activating the endoplasmic reticulum (ER)-mitochondrial axis to induce cell death [30, 31]. Ellagic acid not only inhibits the proliferation of MCF-7 human breast cancer cells by regulating

the transforming growth factor- β (TGF- β)/Smad3 signalling pathway and reducing Rb protein phosphorylation [32] but also inhibits the growth of MDA-MB-231 cells by regulating p-VEGFR2 (vascular endothelial growth factor receptor-2) expression by activating the VEGFR-2 signalling pathway [33]. As a well-known natural anthocyanin, pelargonidin exerts an anti-effect on tumour transformation and apoptosis by inducing Nrf2 signalling pathway activation [34] and inhibiting cyclin-dependent kinase 1 (CDK1) activation [35]. Anthocyanins achieve antitumour effects by suppressing cancer cell proliferation, inducing cancer cell apoptosis, and subsequently preventing the tumour cell invasion and the formation of distant metastases [36, 37]. Petunia extract inhibit the growth of 53% of breast cancer cells when used at concentration of 200 $\mu\text{g}/\text{mL}$ [37–39]. Therefore, traditional Chinese medicine is an important source of drugs for clinical use [18, 19], even when its multicomponent, multitarget, and diverse regulation characteristics do not facilitate the identification of the key compounds and complex interactions in the traditional Chinese medicine formulas. On the other hand, network pharmacology is an advanced, efficient, and suitable method to systemati-

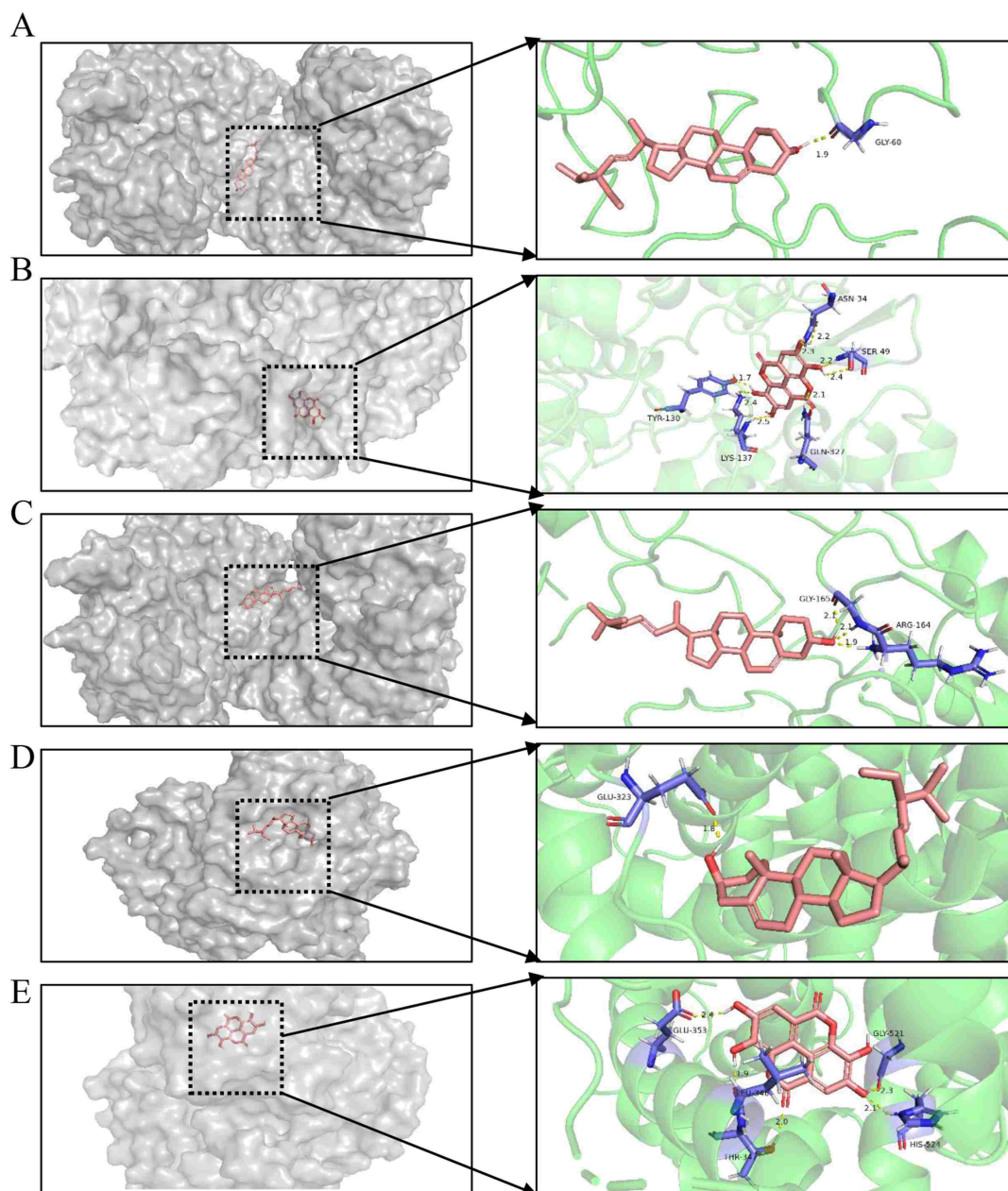


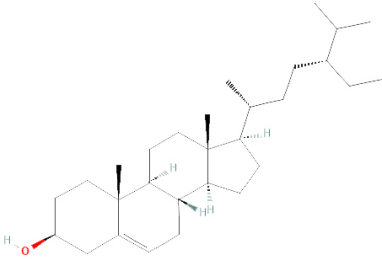
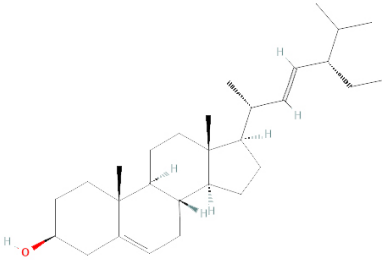
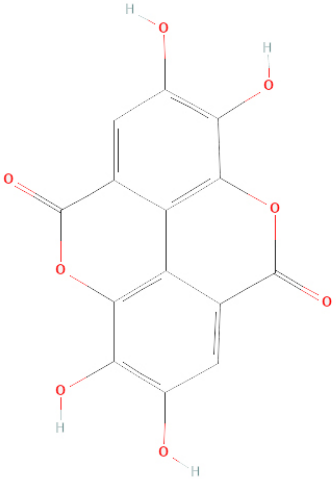
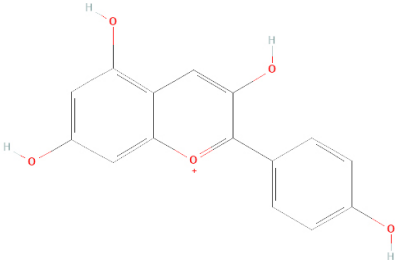
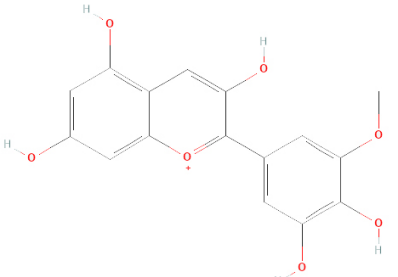
FIGURE 6. Schematic diagram of docking results. (A) CASP3-stigmasterol; (B) PTGS2-ellagic acid; (C) CASP3-sitosterol; (D) ESR1-ellagic acid; and (E) ESR1-stigmasterol.

cally study traditional Chinese medicine compounds [20–22]. Here, we are the first to predict the potential active molecules, targets, and mechanisms of TAFM in the treatment of breast cancer by constructing a traditional Chinese medicine-active ingredients-targets-diseases network and performing molecular docking. The information presented in this study provides a new perspective for breast cancer treatment research and a research direction for the precise treatment of cancer using these compounds.

A total of 38 overlapping targets, including the hub genes *ESR1*, *VEGFA*, *PTGS2*, *HSP90AA1*, and *CASP3*, were identified according to the Venn diagram. *ESR1* encodes oestrogen receptor alpha (ER), and it can transcriptionally regulate the downstream roles of the oestrogen signalling pathway in breast cancer [40]. *ESR1* mutation is the most common cause of resistance to endocrine therapy, and high *ESR1* expression

levels are typically associated with a poor prognosis in patients with ER-positive breast cancer [41, 42]. *VEGFA* is one of the main factors promoting the expansion of the tumour vascular bed, which can manifest as high vascular turnover, poor blood perfusion, and increased leakage. To regulate angiogenesis and vascular permeability, hypoxic tumours and endothelial cells produce a large amount of *VEGFA* and rely on a variety of signalling pathways, including the Phospholipase C extracellular regulated protein kinase (ERK) pathway, the SRC tyrosine family kinase (SFKs) pathway, and the phosphatidylinositol-3-kinase/protein kinase B (PI3K/Akt) pathway [43–45]. As a cancer biomarker, *HSP90AA1* is highly expressed under stimulating conditions, such as trauma, infection, and tumours, and is involved in DNA damage regulation, gene expression, and carcinogenesis [46]. A study discovered that the presence of *HSP90AA1* and other plasma markers could accurately

TABLE 2. Key active component information.

Active Component	Degree	CAS	Structure
Beta-sitosterol	16	83-46-5	
Stigmasterol	16	83-48-7	
Ellagic acid	14	476-66-4	
Pelargonidin	7	7690-51-9	
Petunidin	6	1429-30-7	

CAS: Chemical Abstracts Service.

TABLE 3. Binding energy of active components and key targets.

Compounds	Binding energy/kcal·mol ⁻¹				
	ESR1 (1GWQ)	VEGFA (4KZN)	PTGS2 (5F19)	HSP90AA1 (1BYQ)	CASP3 (3DEI)
Beta-sitosterol	-5.03	-6.82	-4.18	-5.26	-8.53
Stigmasterol	-8.61	-7.18	-4.89	-7.04	-8.86
Ellagic acid	-8.17	-6.21	-8.39	-5.21	-6.65
Pelargonidin	-6.69	-5.86	-7.65	-5.38	-6.45
Petunidin	-6.33	-5.89	-6.94	-4.82	-5.85

ESR1: estrogen receptor alpha; VEGFA: vascular endothelial growth factor A; PTGS2: prostaglandin-endoperoxide synthase 2; HSP90AA1: heat shock protein 90 alpha; CASP3: Caspase 3.

predict the risk of breast cancer metastasis [47]. *CASP3* is a key protease involved in cell apoptosis; hence, it is frequently used as a marker of therapeutic efficacy in cancer [48, 49]. Moreover, tumour cells produce effective growth stimulation signals when activated during apoptosis, and activated *CASP3* is the key executor in cell apoptosis and participates in growth stimulation [50]. The *CASP3*/PKC (protein kinase C)/AKT/VEGF- α axis has been implicated in tumour reconstruction, and *CASP3* or *CASP7* inactivation can weaken colorectal tumour reconstruction and PKC signalling [51]. Altogether, the five hub genes are important in tumorigenesis and the development of breast cancer.

GO analysis results revealed that the effects of TAFM treatment on breast cancer involved multiple biological processes, mainly including drug response, positive regulation of apoptosis, and bidirectional regulation of gene expression. KEGG analysis implicated the following pathways, including cancer-, inflammation-, and infection-related disease pathways. These biological processes and metabolic pathways are closely related to tumour cell proliferation. Cytomegalovirus nucleic acids and proteins play roles in many cancers, including colorectal, prostate, and breast cancers [52]. After 24, 48, and 72 h of human cytomegalovirus infection, the proliferation and viability of HT29 and SW480 parent cells and stem cell-like cells were significantly increased ($p < 0.0001$), and cell migration was promoted [53]. The growth factor IL-17 β can directly promote tumour growth and inhibit apoptosis of 4T1, MDA-MB-231, and EM6 BC cell lines by targeting the immune system [54]. These studies indicate that the efficacy of TAFM was achieved through the synergy of multiple pathways.

5. Conclusion

In this study, we have provided supportive evidence that the potential pharmacological mechanism of TAFM in the treatment of breast cancer encompasses a variety of compounds, multiple targets, and multiple signalling pathways. Among them, the key bioactive agents, including β -sitosterol, stigmasterol, ellagic acid, pelargonidin, and petunidin, potentially exert anti-breast cancer effects by regulating core targets, including the *ESR1*, *VEGFA*, *PTGS2*, *HSP90AA1*, and *CASP3* genes. Although neither *in vivo* nor *in vitro* experiments were conducted due to budget and time constraints, this study provides a research direction for further studies on TAFM in

the treatment of breast cancer.

AUTHOR CONTRIBUTIONS

JY, XZ conceived and designed the analysis. JY, XZ completed the data retrieval. JY, XZ and ZD analyzed the data. JY wrote the paper. JT and ZJ revised the paper. All authors read and approved the final manuscript.

ETHICS APPROVAL AND CONSENT TO PARTICIPATE

Not applicable.

ACKNOWLEDGMENT

Not applicable.

FUNDING

This research was supported by Graduate Research and Innovation Plan of Jiangsu Province (No. KYCX20_1476), the National Natural Science Foundation of China (No.81704083).

CONFLICT OF INTEREST

The authors declare no conflict of interest.

REFERENCES

- [1] Coughlin SS. Epidemiology of breast cancer in women. *Advances in Experimental Medicine and Biology*. 2019; 33: 9–29.
- [2] Sung H, Ferlay J, Siegel RL, Laversanne M, Soerjomataram I, Jemal A, *et al.* Global cancer statistics 2020: GLOBOCAN estimates of incidence and mortality worldwide for 36 cancers in 185 countries. *CA: a Cancer Journal for Clinicians*. 2021; 71: 209–249.
- [3] Li R, Hu X, Shang F, Wu W, Zhang H, Wang Y, *et al.* Treatment of triple negative breast cancer by near infrared light triggered mild-temperature photothermal therapy combined with oxygen-independent cytotoxic free radicals. *Acta Biomaterialia*. 2022; 148: 218–229.
- [4] Wei Y, Guo Y, Lv S. Research on the progress of traditional chinese medicine components and preparations on histone deacetylase inhibitors—like effects in the course of disease treatment. *Journal of Ethnopharmacology*. 2022; 296: 115521.
- [5] Qu J, Liu Q, You G, Ye L, Jin Y, Kong L, *et al.* Advances in ameliorating

- inflammatory diseases and cancers by andrographolide: pharmacokinetics, pharmacodynamics, and perspective. *Medicinal Research Reviews*. 2022; 42: 1147–1178.
- [6] Ramaiah MJ, Tangutur AD, Manyam RR. Epigenetic modulation and understanding of HDAC inhibitors in cancer therapy. *Life Sciences*. 2021; 277: 119504.
- [7] Pengbo Wang, Yunyun Dai, Han Dong, Mengyu Yan, Xiaorong Xie. Summary of research on intervention of chinese medicine in breast cancer treatment. *Chinese Journal of Experimental Traditional Medical Formulae*. 2021; 27: 235–243.
- [8] Ru J, Li P, Wang J, Zhou W, Li B, Huang C, *et al*. TCMSP: a database of systems pharmacology for drug discovery from herbal medicines. *Journal of Cheminformatics*. 2014; 6: 13.
- [9] Stelzer G, Rosen N, Plaschkes I, Zimmerman S, Twik M, Fishilevich S, *et al*. The genecards suite: from gene data mining to disease genome sequence analyses. *Current Protocols in Bioinformatics*. 2016; 54: 1.30.1–1.30.33.
- [10] Amberger JS, Hamosh A. Searching online mendelian inheritance in man (OMIM): a knowledgebase of human genes and genetic phenotypes. *Current Protocols in Bioinformatics*. 2017; 58: 1.2.1–1.2.12.
- [11] Y. Wang, S. Zhang, F. Li, Y. Zhou, Y. Zhang, Z. Wang, *et al*. Therapeutic target database 2020: enriched resource for facilitating research and early development of targeted therapeutics. *Nucleic Acids Research*. 2020; 48: D1031–D1041.
- [12] Wishart DS, Feunang YD, Guo AC, Lo EJ, Marcu A, Grant JR, *et al*. DrugBank 5.0: a major update to the DrugBank database for 2018. *Nucleic Acids Research*. 2018; 46: D1074–D1082.
- [13] Szklarczyk D, Gable AL, Lyon D, Junge A, Wyder S, Huerta-Cepas J, *et al*. STRING v11: protein-protein association networks with increased coverage, supporting functional discovery in genome-wide experimental datasets. *Nucleic Acids Research*. 2019; 47: D607–D613.
- [14] Huang DW, Sherman BT, Lempicki RA. Systematic and integrative analysis of large gene lists using DAVID bioinformatics resources. *Nature Protocols*. 2009; 4: 44–57.
- [15] Burley SK, Berman HM, Bhikadiya C, Bi C, Chen L, Di Costanzo L, *et al*. RCSB protein data bank: biological macromolecular structures enabling research and education in fundamental biology, biomedicine, biotechnology and energy. *Nucleic Acids Research*. 2019; 47: D464–D474.
- [16] Kim S, Chen J, Cheng T, Gindulyte A, He J, He S, *et al*. PubChem in 2021: new data content and improved web interfaces. *Nucleic Acids Research*. 2021; 49: D1388–D1395.
- [17] Li B, Rui J, Ding X, Yang X. Exploring the multicomponent synergy mechanism of banxia xiexin decoction on irritable bowel syndrome by a systems pharmacology strategy. *Journal of Ethnopharmacology*. 2019; 233: 158–168.
- [18] Liu S, Chuang W, Lam W, Jiang Z, Cheng Y. Safety surveillance of traditional chinese medicine: current and future. *Drug Safety*. 2015; 38: 117–128.
- [19] Deyrup ST, Stagnitti NC, Perpetua MJ, Wong-Deyrup SW. Drug discovery insights from medicinal beetles in traditional Chinese medicine. *Biomolecules & Therapeutics*. 2021; 29: 105–126.
- [20] Song X, Zhang Y, Dai E, Du H, Wang L. Mechanism of action of celastrol against rheumatoid arthritis: a network pharmacology analysis. *International Immunopharmacology*. 2019; 74: 105725.
- [21] Ye J, Li L, Hu Z. Exploring the molecular mechanism of action of yinchen wuling powder for the treatment of hyperlipidemia, using network pharmacology, molecular docking, and molecular dynamics simulation. *BioMed Research International*. 2021; 2021: 1–14.
- [22] Lin Y, Shen C, Wang F, Fang Z, Shen G. Network pharmacology and molecular docking study on the potential mechanism of yi-qi-huo-xue-tong-luo formula in treating diabetic peripheral neuropathy. *Journal of Diabetes Research*. 2021; 2021: 1–16.
- [23] Yousef RG, Ibrahim A, Khalifa MM, Eldehna WM, Gobaara IMM, Mehany ABM, *et al*. Discovery of new nicotinamides as apoptotic VEGFR-2 inhibitors: virtual screening, synthesis, anti-proliferative, immunomodulatory, ADMET, toxicity, and molecular dynamic simulation studies. *Journal of Enzyme Inhibition and Medicinal Chemistry*. 2022; 37: 1389–1403.
- [24] V. Kumar, S. Parate, Danishuddin, A. Zeb, P. Singh, G. Lee, *et al*. 3D-QSAR-based pharmacophore modeling, virtual screening, and molecular dynamics simulations for the identification of spleen tyrosine kinase inhibitors. *Frontiers in Cellular and Infection Microbiology*. 2022; 12: 909111.
- [25] Qayed WS, Hassan MA, El-Sayed WM, Rogério A. Silva J, Aboul-Fadl T. Novel azine linked hybrids of 2-indolinone and thiazolidinone scaffolds as CDK2 inhibitors with potential anticancer activity: in silico design, synthesis, biological, molecular dynamics and binding free energy studies. *Bioorganic Chemistry*. 2022; 126: 105884.
- [26] Manayi A, Saeidnia S, Ostad SN, Hadjiakhoondi A, Ardekani MRS, Vazirian M, *et al*. Chemical constituents and cytotoxic effect of the main compounds of *Lythrum salicaria* L. *Z Naturforsch C J Biosci*. 2013; 68: 367–375.
- [27] Ervina M, Poerwono H, Widowati R, Matsunami K, Sukardiman. Bio-selective hormonal breast cancer cytotoxic and antioxidant potencies of *Melia azedarach* L. wild type leaves. *Biotechnology Reports*. 2020; 25: e00437.
- [28] M.S. Zubair, W.M. Alarif, M.A. Ghandourah, S. Anam. A new steroid glycoside from *Begonia* sp.: cytotoxic activity and docking studies. *Natural Product Research*. 2021; 35: 2224–2231.
- [29] Awad AB, Chinnam M, Fink CS, Bradford PG. B-sitosterol activates fas signaling in human breast cancer cells. *Phytomedicine*. 2007; 14: 747–754.
- [30] Y. Ma, G. Li, M. Yu, K. Cao, Q. Li, X. Sun, *et al*. Anti-lung cancer targets of *radix paeoniae rubra* and biological molecular mechanism: network pharmacological analyses and experimental validation. *Oncotargets and Therapy*. 2021; 14: 1925–1936.
- [31] H. Bae, G. Song, W. Lim. Stigmasterol causes ovarian cancer cell apoptosis by inducing endoplasmic reticulum and mitochondrial dysfunction. *Pharmaceutics*. 2020; 12: 488.
- [32] Zhang T, Chen H, Wang L, Bai M, Wang Y, Jiang X, *et al*. Ellagic acid exerts anti-proliferation effects *via* modulation of *tgf-β/smad3* signaling in MCF-7 breast cancer cells. *Asian Pacific Journal of Cancer Prevention*. 2014; 15: 273–276.
- [33] Wang N, Wang Z, Mo S, Loo TY, Wang D, Luo H, *et al*. Ellagic acid, a phenolic compound, exerts anti-angiogenesis effects *via* VEGFR-2 signaling pathway in breast cancer. *Breast Cancer Research and Treatment*. 2012; 134: 943–955.
- [34] Li S, Li W, Wang C, Wu R, Yin R, Kuo H, *et al*. Pelargonidin reduces the TPA induced transformation of mouse epidermal cells—potential involvement of Nrf2 promoter demethylation. *Chemico-Biological Interactions*. 2019; 309: 108701.
- [35] Karthi N, Karthiga A, Kalaiyarasu T, Stalin A, Manju V, Singh SK, *et al*. Exploration of cell cycle regulation and modulation of the DNA methylation mechanism of pelargonidin: insights from the molecular modeling approach. *Computational Biology and Chemistry*. 2017; 70: 175–185.
- [36] Mudd AM, Gu T, Munagala R, Jeyabalan J, Fraig M, Egilmez NK, *et al*. Berry anthocyanidins inhibit intestinal polyps and colon tumors by modulation of Src, EGFR and the colon inflammatory environment. *Oncoscience*. 2021; 8: 120–133.
- [37] Wang G, Fu X, Wang J, Guan R, Sun Y, Tony To S. Inhibition of glycolytic metabolism in glioblastoma cells by Pt3glc combined with PI3K inhibitor *via* SIRT3-mediated mitochondrial and PI3K/Akt-MAPK pathway. *Journal of Cellular Physiology*. 2019; 234: 5888–5903.
- [38] Zhang Y, Vareed SK, Nair MG. Human tumor cell growth inhibition by nontoxic anthocyanidins, the pigments in fruits and vegetables. *Life Sciences*. 2005; 76: 1465–1472.
- [39] Kausar H, Jeyabalan J, Aqil F, Chabba D, Sidana J, Singh IP, *et al*. Berry anthocyanidins synergistically suppress growth and invasive potential of human non-small-cell lung cancer cells. *Cancer Letters*. 2012; 325: 54–62.
- [40] Fowler AM, Salem K, DeGrave M, Ong IM, Rassman S, Powers GL, *et al*. Progesterone receptor gene variants in metastatic estrogen receptor positive breast cancer. *Hormones and Cancer*. 2020; 11: 63–75.
- [41] Györfy B, Lanczky A, Eklund AC, Denkert C, Budczies J, Li Q, *et al*. An online survival analysis tool to rapidly assess the effect of 22,277 genes on breast cancer prognosis using microarray data of 1809 patients. *Breast Cancer Research and Treatment*. 2010; 123: 725–731.
- [42] Gu G, Tian L, Herzog SK, Rechoum Y, Gelsomino L, Gao M, *et al*.

- Hormonal modulation of *ESR1* mutant metastasis. *Oncogene*. 2021; 40: 997–1011.
- [43] Takahashi T. A single autophosphorylation site on KDR/Flk-1 is essential for VEGF-a-dependent activation of PLC-gamma and DNA synthesis in vascular endothelial cells. *The EMBO Journal*. 2001; 20: 2768–2778.
- [44] Sun Z, Li X, Massena S, Kutschera S, Padhan N, Gualandi L, *et al.* VEGFR2 induces c-Src signaling and vascular permeability *in vivo* via the adaptor protein TSA. *Journal of Experimental Medicine*. 2012; 209: 1363–1377.
- [45] Joshi S, Singh AR, Zulcic M, Durden DL. A macrophage-dominant PI3K isoform controls hypoxia-induced HIF1 α and HIF2 α stability and tumor growth, angiogenesis, and metastasis. *Molecular Cancer Research*. 2014; 12: 1520–1531.
- [46] V. Condelli, F. Crispo, M. Pietrafesa, G. Lettini, D.S. Matassa, F. Esposito, *et al.* HSP90 molecular chaperones, metabolic rewiring, and epigenetics: impact on tumor progression and perspective for anticancer therapy. *Cells*. 2019; 8: 532.
- [47] H. Liu, Z. Zhang, Y. Huang, W. Wei, S. Ning, J. Li, *et al.* Plasma *HSP90AA1* predicts the risk of breast cancer onset and distant metastasis. *Frontiers in Cell and Developmental Biology*. 2021; 9: 639596.
- [48] Boland K, Flanagan L, Prehn JH. Paracrine control of tissue regeneration and cell proliferation by Caspase-3. *Cell Death & Disease*. 2013; 4: e725–e725.
- [49] Zhou M, Liu X, Li Z, Huang Q, Li F, Li C. Caspase-3 regulates the migration, invasion and metastasis of colon cancer cells. *International Journal of Cancer*. 2018; 143: 921–930.
- [50] Cheng J, Tian L, Ma J, Gong Y, Zhang Z, Chen Z, *et al.* Dying tumor cells stimulate proliferation of living tumor cells *via* caspase-dependent protein kinase C δ activation in pancreatic ductal adenocarcinoma. *Molecular Oncology*. 2015; 9: 105–114.
- [51] Cheng J, He S, Wang M, Zhou L, Zhang Z, Feng X, *et al.* The Caspase-3/PKC δ /Akt/VEGF-a signaling pathway mediates tumor repopulation during radiotherapy. *Clinical Cancer Research*. 2019; 25: 3732–3743.
- [52] Harkins LE, Matlaf LA, Soroceanu L, Klemm K, Britt WJ, Wang W, *et al.* Detection of human cytomegalovirus in normal and neoplastic breast epithelium. *Herpesviridae*. 2010; 1: 8.
- [53] W.H. Teo, H.P. Chen, J.C. Huang, Y.J. Chan. Human cytomegalovirus infection enhances cell proliferation, migration and upregulation of EMT markers in colorectal cancer-derived stem cell-like cells. *International Journal of Oncology*. 2017; 51: 1415–1426.
- [54] J.S. Nam, M. Terabe, M.J. Kang, H. Chae, N. Voong, Y.A. Yang, *et al.* Transforming growth factor beta subverts the immune system into directly promoting tumor growth through interleukin-17. *Cancer research*. 2008; 68: 3915–3923.

How to cite this article: Jinqing Yang, Xiaochun Zhang, Zhiwei Jiang, Zhengming Deng, Jinhai Tang. Analysis of the drug-target-disease network of trichosanthes-angelica sinensis-frankincense-myrrh in the treatment of breast cancer. *European Journal of Gynaecological Oncology*. 2022; 43(6): 83-95. doi: 10.22514/ejgo.2022.061.